Laser-Induced Thermal Effect on Sensitivity of Scanning Near-Field Optical Microscope Probe

Haw-Long Lee, Yu-Ching Yang, and Win-Jin Chang*

Department of Mechanical Engineering, Kun Shan University, Tainan 710, Taiwan

Received May 13, 2010; accepted July 14, 2010; published online December 20, 2010

In this study, the laser-induced thermal effect on the sensitivity of a scanning near-field optical microscope (SNOM) tapered probe is analyzed. In the analysis, the thermal effect can be considered as an axial force and is dependent on the temperature distribution of the probe. The Rayleigh–Ritz method is used to determine the sensitivity of the probe. According to the analysis, the sensitivity of the first three vibration modes increases when the thermal effect is taken into account. When the contact stiffness is low, the thermal effect on the sensitivity of mode 1 is particularly significant. The sensitivity of mode 1 increases with increasing taper angle and coating thickness of the probe. In addition, the effect of a SNOM probe with three different coating materials, Al, Au, and Ag, on the sensitivity of mode 1 is studied. The result shows that the highest sensitivity is obtained for the probe with an Al coating, whereas it is the lowest with a Au coating.

DOI: 10.1143/JJAP.49.125201

1. Introduction

In recent years, scanning near-field optical microscopy (SNOM) has become one of the major proximal probe technologies. SNOM can be used not only to obtain high resolution images beyond the diffraction limit of light but also to fabricate nanometer-scale structures through material removal, modification, and deposition.[1–5] A tapered optical fiber probe with an opaque metallic coating is the key element of SNOM. It can be used to perform various physical and chemical processes through electromagnetic, optical, or thermal sources.[6–8] During operation, heating of the probe is inevitable owing to laser light absorption, which may increase temperature of the probe in the apical region up to several hundred degrees.[9] The temperature gradient in the probe leads to a gradient of the refraction index which shifts the optical mode.[10]

In SNOM, the distance between the probe and the specimen is controlled by a shear force technique based on the detection of a shift in the frequency of the vibrating probe.[11] However, the frequency shift of the probe can be affected by the thermal effect because of laser light absorption, which leads to a change in sensitivity. Therefore, some researchers have studied the thermal behavior of the SNOM probe. For example, Stahelin *et al.*[12] measured the temperature profile of aluminum-coated fiber tips as a function of optical input power with a micron sized thermocouple. They found that a temperature of up to 470 °C was measured close to the aperture with an optical input power of several mW. Finot *et al.*[13] investigated the thermomechanical behavior of coated tapered fibers using a thermal model and found that the resonance frequency of the tapered fiber was a function of fiber length and coating profile. Lee *et al.*[14] applied a conjugate gradient method to study the temperature distribution of the SNOM probe owing to light absorption.

In general, when a probe scans a sample surface and the probe–sample spacing is sufficiently small (<10 nm), interaction forces between the probe tip and the sample surface are induced. The forces result in a frequency shift. This shift can be used to control distance control via a feedback mechanism acting on the piezo.[15] In SNOM, it is important to have good control of the probe-to-sample distance. The distance is related to the interaction forces and can be estimated by measuring the vibration amplitude of the probe.[16,17] However, the analysis of dynamic responses, including resonant frequency, is complicated, and a precise analysis is difficult, but the responses affect the imaging rate and performance during operation. Therefore, many researchers have developed a growing interest in studying the vibration responses of the SNOM probe.[18–21]

Recently, Lee *et al.*[22] studied the vibration frequency of a SNOM tapered probe owing to the thermal effect. In this study, the laser-induced thermal effect on the sensitivity of a SNOM tapered probe is analyzed. The sensitivity of the probe, based on the contact stiffness between the probe and sample, is derived using Bernoulli–Euler beam theory, including the thermal effect. In addition, the effects of contact stiffness, different coating materials, and thicknesses are studied for different taper angles.

2. Analysis

A SNOM apparatus with a tapered probe is cantilevered at one end, as depicted in Fig. 1. The probe consists of an optical fiber with a metal coating layer t_c to prevent light leakage. The probe has length L, a uniform cylindrical section with radius R_0, a tapered section with taper angle θ, and a tip of radius r_0. The interaction of the probe with the sample is modeled using the spring constant k_l. In addition, the probe is subjected to a thermal force in the axial direction owing to the laser light absorption during operation. The axial force should be included in the vibration analysis of the probe. The lateral vibration of the probe is modeled by a partial differential equation and its transverse displacement Y is dependent on time t and the spatial coordinate X. Bernoulli–Euler beam theory is employed to describe the vibration behavior of the probe. The governing equation of motion for the probe is

$$\frac{\partial^2}{\partial X^2}\left[EI(X)\frac{\partial^2 Y(X,t)}{\partial X^2}\right] - \frac{\partial}{\partial X}\left[P(X)\frac{\partial Y(X,t)}{\partial X}\right] = -\rho A(X)\frac{\partial^2 Y(X,t)}{\partial t^2}, \quad (1)$$

where X is the distance from the fixed end of the probe, E is Young's modulus, $I(X)$ is the area moment of inertia, ρ is the volume density, and $A(X)$ is the circular cross-sectional area

*E-mail address: changwj@mail.ksu.edu.tw

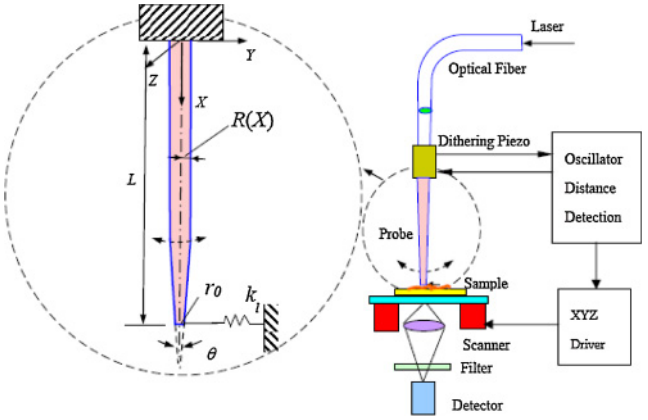

Fig. 1. (Color online) Schematic diagram of SNOM apparatus with a tapered probe cantilevered at one end. The interaction with the sample is modeled using the lateral spring stiffness k_l.

of the probe. $P(X)$ denotes the axial tension force, which depends on the temperature distribution $T(X)$ along the probe length and the thermal expansion coefficient α of the probe. Therefore, the force can be expressed as $P(X) = \alpha EA(X)T(X)$.

The corresponding boundary conditions are

$$Y(0,t) = 0, \tag{2}$$

$$\frac{\partial Y(0,t)}{\partial X} = 0, \tag{3}$$

$$\left[EI(X)\frac{\partial^2 Y(X,t)}{\partial X^2}\right]\Big|_{X=L} = 0, \tag{4}$$

$$\frac{\partial}{\partial X}\left[EI(X)\frac{\partial^2 Y(X,t)}{\partial X^2}\right]\Big|_{X=L} = k_l Y(X,t) + P(X)\frac{\partial Y(X,t)}{\partial x}\Big|_{X=L}. \tag{5}$$

The SNOM probe is assumed to be a cantilever beam fixed at the end of $X = 0$; then the boundary conditions given by eqs. (2) and (3) correspond to the conditions of zero displacement and zero slope at $X = 0$. The boundary condition given by eq. (4) represents the zero moment at $X = L$, and eq. (5) denotes the shear force at $X = L$. The shear force is induced by the thermal effect and the interaction between the probe tip and the material surface. To increase the spatial resolution, the fiber is coated with a metal layer with thickness t_c. Therefore, the coating of the fiber will increase the stiffness and mass of the probe. For a coated probe, $EI(X)$, $\rho A(X)$, and $P(X)$ in the equation of motion should be replaced by the following equivalent values:

$$E_e I_e(X) = E_f I_f(X) + E_c I_c, \tag{6}$$

$$\rho_e A_e(X) = \rho_f A_f(X) + \rho_c A_c, \tag{7}$$

$$P_e(X) = [\alpha_f A_f(X) E_f + \alpha_c A_c(X) E_c] T(X), \tag{8}$$

where the subscripts "f" and "c" refer to the fiber and coating, respectively.

During operation, the probe tip is heated owing to the absorption of laser light, which leads to an increase in the probe temperature. The temperature profile $T(X)$ along the probe length is assumed to be in the following exponential form:[13,23)]

$$T(X) = T_{\max} \exp\left[\sqrt{-\frac{2h}{(R+t_c)k}}(1-X)\right], \tag{9}$$

where $T_{\max}$ is the temperature of the probe tip, $R(X)$ is the radius of the fiber and is assumed to be a function of X, h is the convection coefficient, and k is the thermal conductivity calculated from the two components of the probe as

$$k = \frac{\alpha_c t_c^2 + \alpha_f R^2}{(R+t_c)^2}, \tag{10}$$

where α_f and α_c are the thermal expansion coefficients for the fiber and coating, respectively.

The harmonic solution of the probe can be expressed as

$$Y(X,t) = v(X)e^{i\omega t}. \tag{11}$$

The dimensionless variables are defined as

$$x = \frac{X}{L}, \quad y = \frac{v}{L}, \quad b^2 = \frac{\omega^2 \rho_e A_0 L^4}{E_e I_0}, \quad p(x) = \frac{P_e(x)L^2}{E_e I_0}$$
$$\beta = \frac{k_l L^3}{E_e I_0}, \quad \zeta(x) = \frac{\rho_e A_e(x)}{\rho_e A_0}, \quad \xi(x) = \frac{E_e I_e(x)}{E_e I_0} \tag{12}$$

where $E_e I_0$ and $\rho_e A_0$ are the equivalent stiffness and the mass of the coated probe at the end of $X = 0$, respectively. On the other hand, b, β, and $p(x)$ denote the dimensionless frequency, contact stiffness, and axial tension force induced by temperature changes, respectively.

Substituting the harmonic solution given by eq. (11) into eqs. (1)–(5) and using the dimensionless variables given by eq. (12), the governing equation and the associated boundary conditions can be simplified to the following dimensionless differential equations and boundary conditions:

$$\frac{d^2}{dx^2}\left[\xi(x)\frac{d^2 y(x)}{dx^2}\right] - p(x)\frac{d^2 y(x)}{dx^2} - b^2\zeta(x)y(x) = 0, \tag{13}$$

$$y(0) = 0, \quad y'(0) = 0, \quad y''(1) = 0,$$

$$\frac{d}{dx}\left[\xi(1)\frac{d^2 y(1)}{dx^2}\right] = ky(1) + p(1)y'(1). \tag{14}$$

Since the parameters of $\xi(x)$, $\zeta(x)$, and $p(x)$ in eq. (13) are dependent on the position x along the coated probe, the Rayleigh–Ritz method[24)] is used to determine the natural frequency. In order to solve eq. (13) by the Rayleigh–Ritz method, we set

$$y = \sum_{i=1}^{n} u_i \gamma_i(x), \tag{15}$$

where u_i are constants, and the admissible functions are $\gamma_i(x)$ which required to satisfy the geometric boundary conditions but need not satisfy the natural boundary conditions. In this calculation, the admissible functions, $\gamma_i(x) = x^i$, $i = 1, 2, 3, \ldots, 10$, were chosen. By substituting eq. (15) into eqs. (13), and (14), then applying the Rayleigh quotient, the following eigenvalue problem can be obtained:

$$Ku = b^2 Mu, \tag{16}$$

where u is the eigenvector of the expansion coefficients and

Table I. Physical properties of selected materials for a SNOM tapered probe.[13,25)]

	E (GPa)	ρ (g/cm^3)	α (10^{-6} K^{-1})	k (Wm^{-1}·K^{-1})
SiO_2	60.0	2.2	5.0	17.0
Au	78.5	19.3	14.1	317
Al	70.6	2.7	23.5	240
Ag	71.0	10.5	19.0	429

$$K_{ij} = \int_0^1 \left[\xi(x) \frac{d^2\gamma_i(x)}{dx^2} \frac{d^2\gamma_j(x)}{dx^2} + p(x) \frac{d\gamma_i(x)}{dx} \frac{d\gamma_j(x)}{dx} \right] dx - \beta\gamma_i(1)\gamma_j(1), \quad (17)$$

$$M_{ij} = \int_0^1 \zeta(x)\gamma_i(x)\gamma_j(x)\, dx. \quad (18)$$

The derivative of the eigenvalue problem, eq. (16), is then taken with respect to β. Subsequently, owing to the fact that the mass matrix M does not depend explicitly on β, and assuming the change in the eigenvector in response to small changes in stiffness is negligible, then we can obtain the following equation:

$$\frac{\partial K}{\partial \beta} u = 2b \frac{\partial b}{\partial \beta} Mu. \quad (19)$$

Finally, the normalization condition $u^{\mathrm{T}}Mu = 1$ is introduced, the normalized flexural sensitivity, S, can then be expressed as

$$S = \frac{\partial b}{\partial \beta} = \frac{1}{2b} u^{\mathrm{T}} \frac{\partial K}{\partial \beta} u. \quad (20)$$

When the contact stiffness is given, the eigenfrequencies and the corresponding eigenvectors can be found from eq. (16), and then the flexural sensitivity for each vibrational mode can be obtained from eq. (20).

3. Results and Discussion

The main purpose of this study is to examine the effects of probe dimensions, coating materials, and contact stiffness on the sensitivity of the vibration modes of a SNOM probe subjected to the thermal effect. In the analysis, we assume that the probe consists of an optical fiber of SiO_2 and a metal coating.[13)] In order to study the effect of relative parameters on the resonant frequency, the geometric and material parameters are listed in Table I.[13,25)] The other parameters are as follows: $R_0 = 50\,\mu\mathrm{m}$, $r_0 = 30\,\mathrm{nm}$, $L = 1600\,\mu\mathrm{m}$, $t_c = 100\,\mathrm{nm}$, $\alpha = 12^\circ$, $T_{\max} = 230\,^\circ\mathrm{C}$, and $h = 1000\,\mathrm{W/(m^2{\cdot}K)}$.[12,13,23)] During operation, the absorption of laser light by the metal coating heats up the probe and leads to the increase in probe temperature. The temperature is related to the taper angle of the probe.[13)] Figure 2 shows the temperature distribution computed using eq. (9) for three taper angles. According to the equation, the maximum temperature at the probe tip is 230 °C. The temperature decreases exponentially with increasing distance from the probe tip. The minimum temperature is the same for each taper angle because of the sufficient length of the probe. When the opening angle is smaller, the temperature distribution in the probe is lower owing to the larger contact area with ambient air.

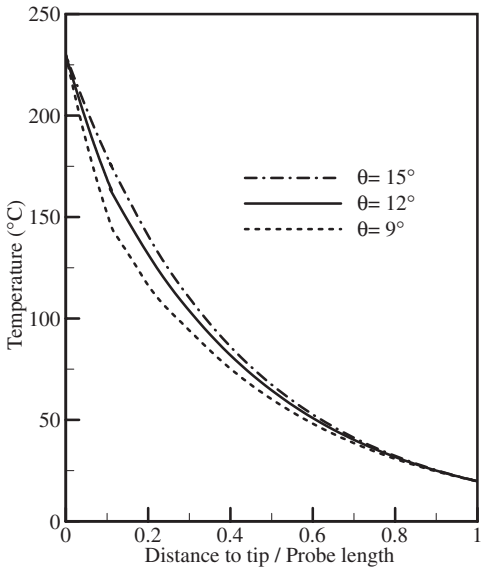

Fig. 2. Temperature distribution of a SNOM probe for different taper angles.

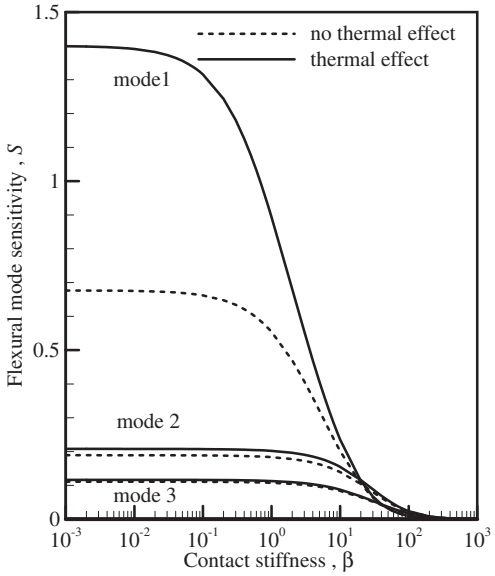

Fig. 3. Thermal effect on the vibration sensitivity of different modes for a SNOM probe with an Al coating of 100 nm thickness and with a taper angle of 12°.

The sensitivity of the probe can be affected by the contact stiffness at the boundary. The sensitivities of the first three modes of flexural vibration for a SNOM probe with an Al coating of 100 nm thickness and with a taper angle of 12° are shown in Fig. 3. Here, the sensitivity is defined as the change in frequency with contact stiffness. From the figure, it can be seen that the probe is sensitive to changes in the contact stiffness, especially for mode 1. Each mode has a different sensitivity to variations in surface stiffness. The sensitivity of the probe decreases as the contact stiffness increases. When the contact stiffness is low, the low-order vibration modes are more sensitive than the high-order modes, and the mode 1 is the most sensitive. According to a previous study,[22)] the vibration frequency increased

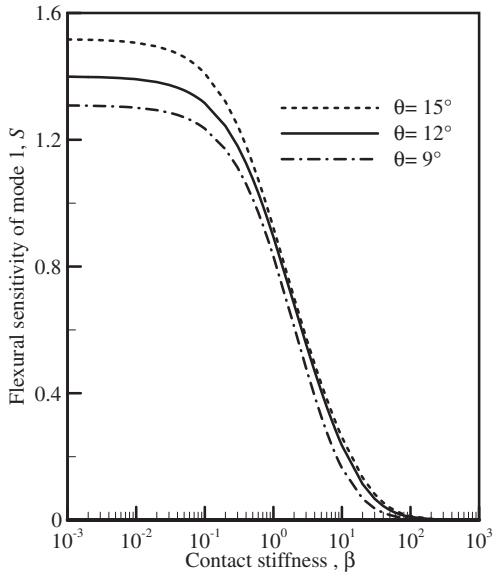

Fig. 4. Vibration sensitivity of mode 1 for a SNOM probe with an Al coating of 100 nm thickness for different taper angles.

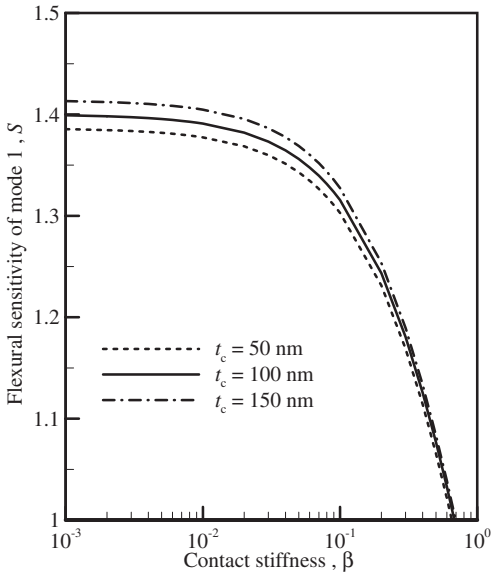

Fig. 5. Vibration sensitivity of mode 1 for a SNOM probe with an Al coating and a taper angle of 12° for different coating thicknesses.

when the thermal effect was considered. Therefore, the sensitivity increases when the thermal effect is taken into account in the analysis. The thermal effect on the sensitivity is obvious, especially when the contact stiffness is low for mode 1.

It is known that the optical transmission efficiency of the SNOM probe strongly depends on the taper angle. The vibration behaviors of the probe are also related to the taper angle. Figure 4 shows the sensitivities of mode 1 for a SNOM probe with an Al coating of 100 nm thickness for different taper angles. The temperature distribution for each taper angle is shown in Fig. 2. A high-temperature distribution of the probe results in a large axial tension force, which results in a large change in frequency. Therefore, it can be seen that the sensitivity of mode 1 increases with increasing taper angle. The effect of the taper angle on the sensitivity is significant when the contact stiffness is low.

The effect of different coating thicknesses on the sensitivity of mode 1 for a SNOM probe with an Al coating and with a taper angle of 12° is shown in Fig. 5. The probe with a thicker coating layer causes less light leakage, which leads to a higher temperature distribution along the probe axis. According to the preceding discussion, the sensitivity of the probe increases owing to a large thermal effect. Therefore, it can be seen from the figure that the sensitivity of mode 1 increases with increasing coating thickness.

Gold, silver, or aluminum is often used for coating the probe to avoid light leakage. In order to study the effect of a SNOM probe with these coating materials on the sensitivity, the sensitivity of mode 1 for a probe with a coating thickness of 100 nm and with a taper angle of 12° is shown in Fig. 6. It can be seen that the highest sensitivity is obtained for the probe with an Al coating, and the lowest sensitivity is obtained for that with a Au coating. This is because the stiffness-to-weight ratio E/ρ of the probe is related to its resonant frequency and sensitivity. Al has the highest E/ρ among the three materials, whereas Au has the lowest.

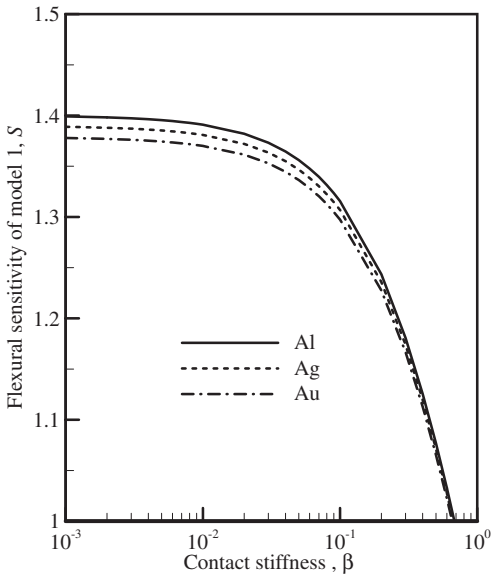

Fig. 6. Vibration sensitivity of mode 1 for a SNOM probe with a coating of 100 nm thickness and a taper angle of 12° for different coating materials.

4. Conclusions

In this study, the Rayleigh–Ritz method was used to analyze the sensitivity of a SNOM tapered probe under the laser-induced thermal effect. On the basis of the analysis, the results showed that the sensitivity of the first three vibration modes increased when the thermal effect was taken into account. The thermal effect on the sensitivity of mode 1 was particularly obvious when the contact stiffness was low. Increasing the taper angle and coating thickness increased the sensitivity of mode 1. In addition, the probe with an Al coating showed the highest sensitivity, and that with a Au coating showed the lowest.

Acknowledgment

The authors wish to thank the National Science Council of the Republic of China in Taiwan for providing financial support for this study under Projects NSC 99-2221-E-168-019 and NSC 99-2221-E-168-031.

1) A. Dereux, C. Girard, C. Chicanne, F. G. Colas, T. David, E. Bourillot, Y. Lacroute, and J. Weeber: Nanotechnology **14** (2003) 935.
2) J. H. Kim and K. B. Song: Micron **38** (2007) 409.
3) A. A. Tseng: Opt. Laser Technol. **39** (2007) 514.
4) J. W. Kingsley, S. K. Ray, A. M. Adawi, G. J. Leggett, and D. G. Lidzey: Appl. Phys. Lett. **93** (2008) 213103.
5) J. Lamela, G. Lifante, T. P. J. Han, F. Jaque, A. García-Navarro, J. Olivares, and F. Agulló-López: Appl. Surf. Sci. **255** (2009) 3918.
6) U. Hohenester: Physica E **35** (2006) 229.
7) A. V. Goncharenko, H. C. Chang, and J. K. Wang: Ultramicroscopy **107** (2007) 151.
8) T. P. J. Han, F. Jaque, J. Lamela, D. Jaque, G. Lifante, F. Cusso, and A. A. Kamiskii: J. Phys.: Condens. Matter **21** (2009) 042201.
9) A. Ambrosio, O. Fenwick, F. Cacialli, R. Micheletto, Y. Kawakami, P. G. Gucciardi, D. J. Kang, and M. Allegrini: J. Appl. Phys. **99** (2006) 084303.
10) S. Vignolini, F. Intonti, L. Balet, M. Zani, F. Riboli, A. Vinattieri, D. S. Wiersma, M. Colocci, L. Li, M. Francardi, A. Gerardino, A. Fiore, and M. Gurioli: Appl. Phys. Lett. **93** (2008) 023124.
11) K. Lindfors, M. Kapulainen, P. Ryytty, and M. Kaivola: Opt. Laser Technol. **36** (2004) 651.
12) M. Stahelin, M. A. Bopp, G. Tarrach, A. J. Meixner, and I. Zschokke-Granacher: Appl. Phys. Lett. **68** (1996) 2603.
13) E. Finot, Y. Lacroute, E. Bourillot, V. Rouessac, and J. Durand: J. Appl. Phys. **95** (2004) 5137.
14) H. L. Lee, W. J. Chang, W. L. Chen, and Y. C. Yang: Ultramicroscopy **107** (2007) 656.
15) K. Taniguchi and Y. Kanemitsu: Jpn. J. Appl. Phys. **44** (2005) 575.
16) H. Heinzelmann and D. W. Pohl: Appl. Phys. A **59** (1994) 89.
17) L. Aigouy, B. Samson, G. Julié, V. Mathet, N. Lequeux, C. N. Allen, H. Diaf, and B. Dubertret: Rev. Sci. Instrum. **77** (2006) 063702.
18) T. H. Fang and W. J. Chang: Opt. Laser Technol. **35** (2003) 267.
19) J. M. Kim, T. Ohtani, and H. Muramatsu: Surf. Sci. **549** (2004) 273.
20) W. J. Chang and T. H. Fang: Phys. Lett. A **348** (2006) 260.
21) J. Liu, A. Callegari, M. Stark, and M. Chergui: Ultramicroscopy **109** (2008) 81.
22) H. L. Lee, W. J. Chang, Y. C. Yang, and S. S. Chu: Appl. Phys. B **97** (2009) 653.
23) L. Thiery and N. Marini: Ultramicroscopy **94** (2003) 49.
24) L. Meirovitch: *Analytical Methods in Vibrations* (Macmillan, New York, 1967).
25) Y. A. Cengel: *Heat Transfer* (McGraw-Hill, New York, 2003).